X-ray Analysis of the Structure of the Thermotropic Copolyester XYDAR†

J. Blackwell,* H.-M. Cheng, and A. Biswas

Department of Macromolecular Science, Case Western Reserve University, Cleveland, Ohio 44106-2699. *Received March 27, 1987*

ABSTRACT: The structure of the thermotropic copolyester prepared from *p*-hydroxybenzoic acid (HBA), terephthalic acid (TPA), and biphenol (BP) has been investigated by X-ray diffraction methods. This chemical formulation is the basis of the XYDAR family of resins. X-ray fiber diagrams for four HBA/TPA/BP comonomer ratios show high orientation and the presence of three-dimensional order. The meridional region contains a series of aperiodic maxima that shift in position with the composition. These are reproduced in predictions of the scattering intensity for a nematic array of chains of completely random monomer sequence. The polymer chains have highly extended conformations, as a result of the linearity of the linkage bonds and the planarity of the aromatic and carboxyl groups. The chains are modeled first as an array of points separated by the appropriate monomer lengths and subsequently via an atomic model, in which the monomer atomic coordinates are attached at each point residue. This leads to good agreement in terms of the position and intensity of the meridional intensity maxima, which is further improved when the effect of chain nonlinearity is incorporated in the calculations, which leads to broadening of the predicted peak at $d = 2.1$ Å. Analysis of models with nonrandom sequence distributions shows that all but minimal blockiness can be ruled out by the X-ray data. The positions of the meridional maxima are unaffected by thermal annealing, and hence the heat treatment does not appear to affect the monomer sequence distribution.

Introduction

This paper describes X-ray analysis of the structure of the wholly aromatic thermotropic copolyesters prepared from *p*-hydroxybenzoic acid (HBA), terephthalic acid (TPA), and biphenol (BP). This formulation is the basis for the XYDAR family of high-temperature, high-performance resins: the properties of these copolymers are described elsewhere.[1,2] The structural anaslysis follows on from our work on other wholly aromatic copolyester and copolyamide systems,[3-6] notably the copolymer of HBA and 2-hydroxy-6-naphthoic acid (HNA). As was the case for the latter copolymers, X-ray fiber diffraction patterns of copoly(HBA/TPA/BP) exhibit a series of aperiodic meridional maxima (along the fiber axis direction); i.e., these maxima do not occur at orders of a simple repeat. The positions (Bragg *d* spacings) of these maxima also shift in systematic manner with the comonomer mole ratio. Such features are inconsistent with extensive block copolymer character. The analogous copolyesters examined previously also give rise to aperiodic meridional data,[3,7] which we have shown point to a completely random comonomer sequence. In this paper we have investigated the meridional data for copoly(HBA/TPA/BP) in terms of the sequence distribution. We have also compared data for as-spun and annealed fibers to investigate possible changes in microstructure as a result of heat treatment.

Experimental Section

X-ray Diffraction. Specimens of copoly(HBA/TPA/BP) were supplied by Dartco Manufacturing Inc., Augusta, GA, in the form of melt-spun fibers for four different HBA/TPA/BP mole ratios: 33/33/33, 50/25/25, 60/20/20, and 72/14/14. The fibers were examined in the as-drawn state and after annealing at 354 °C for 1 h. Specimens for X-ray analysis were prepared as parallel bundles of ~50 fibers. X-ray fiber diagrams were recorded on Kodak no-screen film using Ni-filtered Cu Kα radiation and a Searle toroidal focusing camera. The *d* spacings were calibrated with calcium fluoride.

X-ray data were also recorded for an oriented molded specimen of the 50/25/25 copolymer, also supplied by Dartco. This specimen was part of a 6 in. × 6 in. × $^1/_8$ in. plaque processed by injection molding (full edge gate) at 400 °C. A piece $^1/_2$ in. × 1 in. was cut from the center of the plaque and ground to approximately one-third of the original thickness by removal of the top and bottom surface layers. The specimen showed high orientation of the chain axes perpendicular to the fill direction in the mold. X-ray patterns were recorded on film, with the chain axis direction perpendicular to the beam, and then tilted at the appropriate angle (θ) for successive meridional maxima. These patterns were scanned by using an Optronics densitometer to record the meridional intensity profiles. Meridional data were also recorded as a $\theta/2\theta$ diffractometer scan, using a Phillips PN 3550/10 diffractometer in the transmission mode.

Model Building. A model of a short chain segment with a typical random comonomer sequence is shown in Figure 1a. The chain can be seen to have an extended conformation, such that the axial advance per monomer is approximately equal to the residue lengths. In the model used here, the lengths of the HBA, TPA, and BP residues are 6.35, 7.15, and 9.86 Å, respectively, measured from ester oxygen to ester oxygen. The model was constructed by using standard bond lengths and angles, and the planar aromatic and ester groups are inclined at 30°.

The intensity on the meridian, $I(Z)$, depends on the projection of the structure on the fiber axis. If we approximate each monomer in the chain in Figure 1a to a point, positioned at the ester oxygen, then the axial projection of the chain is represented by a linear array of points separated by the corresponding monomer lengths, as in Figure 1b. This can then be converted to an atomic model for the chain, by adding the projection of the atomic structure of the appropriate monomer at each ester oxygen, as in Figure 1c. For the actual chain in three dimensions, the conformation depends on the torsion angles that define the mutual orientation of adjacent monomers. However, the projection of the extended chain onto the fiber axis will be approximately independent of torsion angles, due to the fact that the aromatic–ester bonds are approximately parallel to the chain axis.

Prediction of Meridional Intensity, $I(Z)$. If the structure is modeled as a nematic array of parallel copolymer chains, then the meridional intensity is derived from the scattering of a single "average" chain. We have shown[8,9] that the extended infinite copolymer chain can be modeled as a one-dimensional paracrystal. The meridional intensity, $I(Z)$, for a chain of point monomers is derived as the Fourier transform of the autocorrelation function, $Q(z)$, that defines the neighbor probability of the point monomers. $Q(z)$ is zero except at $z = z_l$, i.e. at allowed combinations of the monomer lengths. $I(Z)$ is given by

$$I(Z) = F[Q(z)] = \sum_l Q(z_l) \exp(2\pi i Z z_l) \quad (1)$$

For an infinite chain, the summation in eq 1 has the following closed form:

$$I(Z) = 1 + 2\,\mathrm{Re}\left[\frac{\mathbf{H}_1(Z)}{1 - \mathbf{H}_1(Z)}\right] \quad (2)$$

† Registered trademark of Dartco Manufacturing Inc.

0024-9297/88/2221-0039$01.50/0

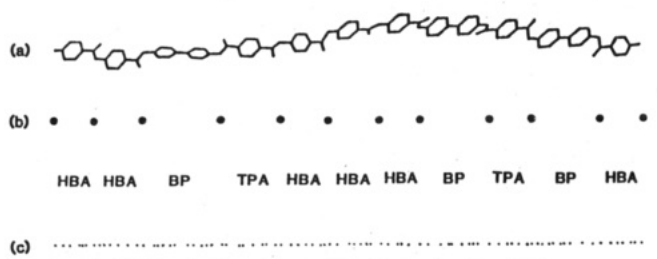

Figure 1. (a) Projection of a model of a typical random sequence of copoly(HBA/TPA/BP). (b) Point residue approximation of the chain in (a). (c) Atomic model for the above sequence. Hydroxybenzoic acid, terephthalic acid, and biphenol are abbreviated to HBA, TPA, and BP, respectively.

where Re designates the real component and $\mathbf{H}_1(Z)$ is the Fourier transform of the first nearest-neighbor probability function. $\mathbf{H}_1(Z)$ can be written as

$$\mathbf{H}_1(Z) = \sum_A \sum_B H_{AB}(Z) \tag{3}$$

where the $H_{AB}(Z)$ terms are the components for the AB nearest-neighbor pairs. Each $H_{AB}(Z)$ is a product of composition and phase terms which depend on the monomer proportions (p_A, p_B, ...), the allowed chemical combinations, and the monomer axial lengths. In the case of copoly(HBA/TPA/BP), the HBA monomer has a sense, unlike TPA and BP which have symmetrical structures, and thus in effect there are four monomers: up-HBA, down-HBA, TPA, and BP. These are further approximated to B, D, T and P, respectively. The proportions of up- and down-HBA are taken as half the total HBA content.

Out of 16 possible monomer pairs, only eight are chemically feasible: for example TPA can react only with BP or the hydroxyl end of HBA. $\mathbf{H}_1(Z)$ can be conveniently written in matrix form.

$$\mathbf{H}_1(Z) = \begin{bmatrix} H_{BB}(Z) & H_{BT}(Z) & 0 & 0 \\ 0 & 0 & H_{TP}(Z) & H_{TD}(Z) \\ H_{PB}(Z) & H_{PT}(Z) & 0 & 0 \\ 0 & 0 & H_{DP}(Z) & H_{DD}(Z) \end{bmatrix} \tag{4}$$

The nonallowed pairs are denoted by the zeros. This matrix can be written as the product of three components:

$$\mathbf{H}_1(Z) = \mathbf{P}\cdot\mathbf{M}\cdot\mathbf{X}(Z) \tag{5}$$

where

$$\mathbf{P} = \begin{bmatrix} p_B & 0 & 0 & 0 \\ 0 & p_T & 0 & 0 \\ 0 & 0 & p_P & 0 \\ 0 & 0 & 0 & p_D \end{bmatrix} \quad \mathbf{M} = \begin{bmatrix} M_{BB} & M_{BT} & 0 & 0 \\ 0 & 0 & M_{TP} & M_{TD} \\ M_{PB} & M_{PT} & 0 & 0 \\ 0 & 0 & M_{DP} & M_{DD} \end{bmatrix}$$

$$\mathbf{X} = \begin{bmatrix} X_B(Z) & 0 & 0 & 0 \\ 0 & X_T(Z) & 0 & 0 \\ 0 & 0 & X_P(Z) & 0 \\ 0 & 0 & 0 & X_D(Z) \end{bmatrix}$$

$X_B(Z) = \exp(2\pi i Z z_B)$, where z_B is the length of monomer B. M_{BB} is the combination probability for the BB monomer pair and is defined as $M_{BB} = 2p_B r_{BB}$. In a completely random copolymer, $r_{BB} = 1$ and $M_{BB} = 2p_B$. r_{BB} can be varied from unity to simulate nonrandom sequence distributions as will be discussed later in this paper. $I(Z)$ can now be written

$$I(Z) = 1 + \sum_A \sum_B 2p_A \text{ Re } [T_{AB}(Z)] \tag{6}$$

where $T_{AB}(Z)$ is an element of the matrix $\mathbf{T}(Z)$ corresponding to the pair AB, and $\mathbf{T}(Z)$ is defined as

$$\mathbf{T}(Z) = \frac{\mathbf{MX}(Z)}{\mathbf{I} - \mathbf{MX}(Z)} \tag{7}$$

and $\mathbf{I}$ is the unity matrix.

When we consider an atomic model, the effects of intraresidue interferences are included by multiplying the element $T_{AB}(Z)$ in matrix $\mathbf{T}(Z)$ by $F_{AB}(Z)$, the Fourier transform of the cross-convolution of monomers A and B. Equation 5 becomes

$$\mathbf{I}(Z) = \sum_A p_A F_{AA}(Z) + \sum_A \sum_B 2p_A \text{ Re } [F_{AB}(Z) T_{AB}(Z)] \tag{8}$$

where

$$F_{AB}(Z) = \sum_j \sum_k f_{A,j} f_{B,k} \exp[2\pi i Z (z_{B,k} - z_{A,j})] \tag{9}$$

The subscript pairs A,j and B,k designate the jth atom in residue A and the kth atom in residue B when both residues have the same origin; f is the atomic scattering factor and z is the axial atomic coordinate.

In the model defined above it is assumed that the axial projections of the residues are constant for each monomer type. In any real chain there will be significant nonlinearity, as can be seen in Figure 1a, and hence the residue projections will not be identical for each monomer type, only approximately so. The distributions of axial lengths for the three monomers are estimated by setting up a large number of random chains by computer and then obtaining histograms of the actual axial lengths. These distributions are then incorporated into the calculations of $I(Z)$ by replacing the terms in the $\mathbf{X}(Z)$ matrix by the summations $X_A(Z) = \sum p_{i,A} \exp(2\pi i Z z_{i,A})$, where $p_{i,A}$ is the fraction of the total content of monomer A which has axial length $z_{i,A}$. When we move to an atomic model, in principle separate $F_{AB}(Z)$ terms need to be computed for each set of residue lengths for monomers A and B. However, the $F_{AB}(Z)$ functions vary only slowly with Z and use of $F_{AB}(Z)$ terms calculated for a single combination of residue lengths is an adequate approximation. Introduction of this distribution leads to a more realistic model for the chain and allows for calculation of a correlation length for the extended conformation, based on the width of certain invariant peaks in $I(Z)$.

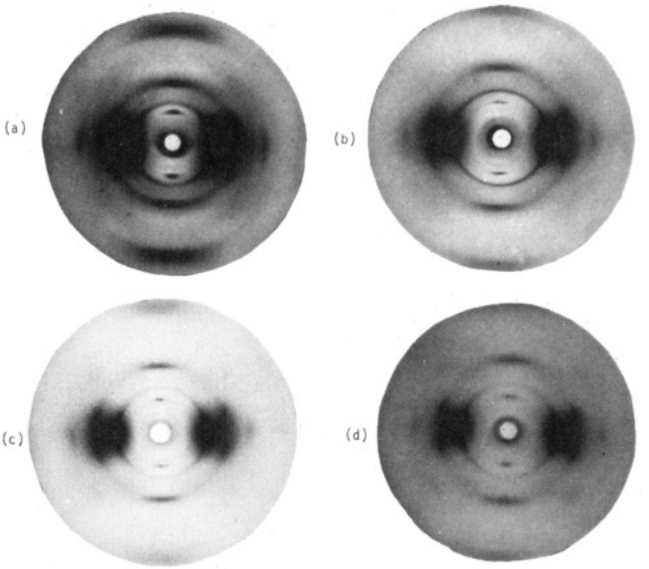

Figure 2. X-ray fiber diagrams of as-drawn copoly(HBA/TPA/BP) in the following monomer ratios: (a) 33/33/33; (b) 50/25/25; (c) 60/20/20; (d) 72/14/14.

Results and Discussion

X-ray Fiber Diagrams. The X-ray fiber diagrams for as-drawn and annealed fiber preparations of the 33/33/33, 50/25/25, 60/20/20, and 72/14/14 copolymers are shown in Figure 2a–d and 3a–d. The fiber axis is vertical for all diffraction patterns. Figure 4 shows the X-ray patterns of the core of the molded plaque, taken with the chain axis perpendicular to the beam and then inclined at 21.5° to that direction.

The X-ray data consist of a series of intensity maxima that appear as relatively short arcs, indicating a high degree of orientation parallel to the fiber axis. A number of sharp Bragg reflections, both on and off the equator, point to the presence of three-dimensional order. These reflections are

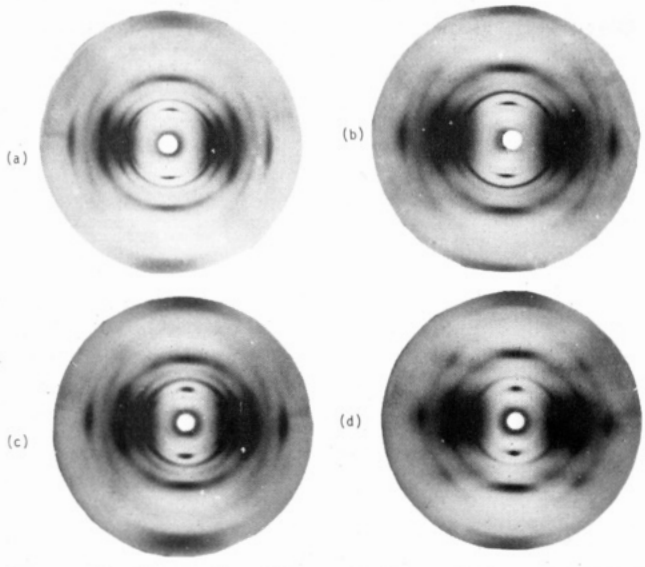

Figure 3. X-ray fiber diagrams of annealed copoly(HBA/TPA/BP) in the following monomer ratios: (a) 33/33/33; (b) 50/25/25; (c) 60/20/20; (d) 72/14/14.

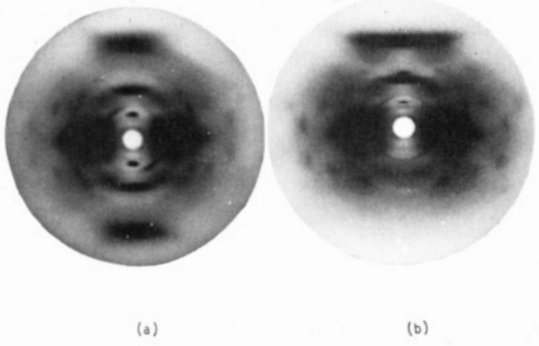

Figure 4. X-ray diffraction patterns of the core of a molded plaque: (a) the chain axis is perpendicular to the X-ray beam; (b) the chain axis is inclined at 21.5° from the plane perpendicular to the beam.

more numerous in the case of annealed specimens. These data indicate that polymorphic structures can occur for these copolymers; one form is present for the as-drawn state, whereas the annealed fibers appear to contain two forms. This has been discussed elsewhere[10] and will also be the subject of a future publication.

Our aim in the present work is to derive a model for the polymer chains, which depends on the scattering along the meridian. Table I shows the d spacings of the meridional maxima for all four copolymer compositions, both as-drawn and annealed. Four maxima are seen in the fiber diagrams of the specimens when approximately perpendicular to the beam. A fifth meridional at $d \cong 2.9$ Å is resolved on tilting three of the specimens (ratios 33/33/33, 50/25/25, and 60/20/20): this fifth meridional at $d = 2.92$ Å can be seen in Figure 4 for the 50/25/25 composition. In the case of the 72/14/14 composition, a shoulder at lower d spacing is seen on the maximum at $d = 3.1$ Å.

Examination of the data in Table I shows that the meridional maxima are both aperiodic and different for all four compositions. The differences between compositions are most apparent from the d spacing of the first maximum, which shifts from 7.7 to 6.6 Å as the content of HBA increases from 33 to 72%. The second and third maxima are more intense and hence can be measured more accurately. These shift from 5.77 to 5.93 Å and from 3.27 to 3.11 Å, respectively, over the same composition range. The very strong peak at 2.08 ± 0.03 Å remains constant

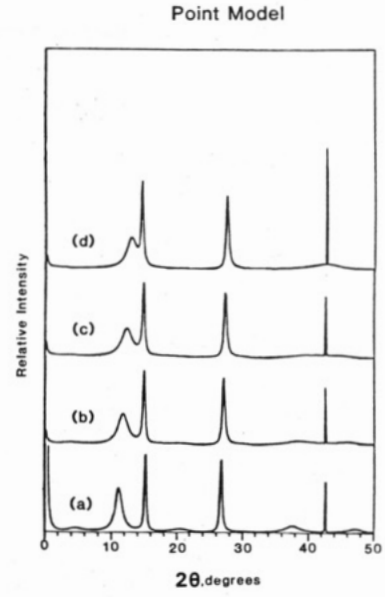

Figure 5. Point model calculations of the meridional intensity distribution for four different monomer ratios of copoly(HBA/TPA/BP): (a) 33/33/33; (b) 50/25/25; (c) 60/20/20; (d) 72/14/14.

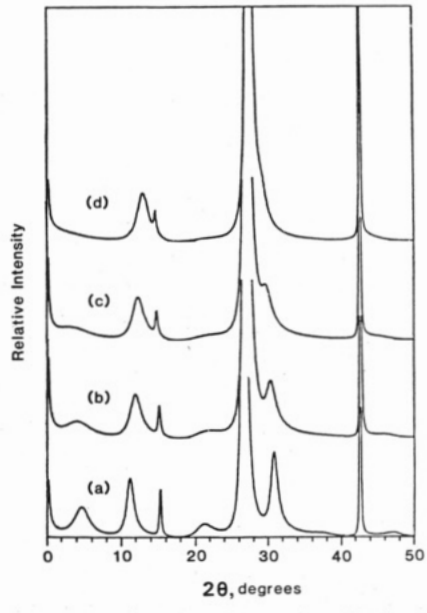

Figure 6. Calculated meridional intensity distribution for four copoly(HBA/TPA/BP) ratios using the atomic model: (a) 33/33/33; (b) 50/25/25; (c) 60/20/20; (d) 72/14/14.

throughout. The figures quoted are for the as-spun specimens. The data for the annealed specimens are within experimental error of those for as-spun in all cases. The aperiodicity of the maxima suggests a random sequence distribution, which will be tested below.

Intensity Calculations. Figures 5 and 6 show the computed meridional intensity for infinite chains of point and atomic monomers for the four HBA/TPA/BP compositions. These data utilized a model for the chain with fixed residue lengths equal to their maximum values, i.e. the ester oxygen–ester oxygen distances. The d spacings of the calculated peaks are compared with the experimental data in Table I.

It can be seen that there is good agreement between the observed and calculated d spacings in all cases: for most maxima the agreement is within experimental error. The shifts in the positions with composition are also predicted in the same systematic manner as is observed. Looking

Table I
d Spacings of Observed and Calculated Meridional Intensity Maxima for Copoly(HBA/TPA/BP)

monomer mole ratio HBA/TPA/BP	exptl *d* spacings, Å		calcd *d* spacings, Å		
	as drawn	annealed	point model	atomic model	distributn
33/33/33	7.7 ± 0.02	7.8 ± 0.2	7.94	7.88	7.76
	5.77 ± 0.05	5.78 ± 0.05	5.82	5.82	5.72
	3.27 ± 0.05	3.29 ± 0.05	3.33	3.34	3.28
	2.87 ± 0.02	2.88 ± 0.02	2.92	2.90	2.85
	2.08 ± 0.03	2.07 ± 0.03	2.12	2.12	2.08
50/25/25	7.3	7.3	7.52	7.47	7.30
	5.82	5.85	5.96	5.92	5.81
	3.20	3.24	3.30	3.30	3.23
	2.90	2.93		2.95	2.90
	2.05	2.05	2.12	2.12	2.08
60/20/20	7.0	6.9	7.20	7.14	7.00
	5.90	5.91	6.03	5.99	5.89
	3.15	3.18	3.28	3.28	3.21
	2.96	2.98		3.01	2.95
	2.05	2.07	2.12	2.12	2.08
72/14/14	6.6	6.6	6.85	6.81	6.67
	5.93	5.97	6.10	6.10	5.99
	3.11	3.12	3.24	3.24	3.19
	2.05	2.04	2.12	2.12	2.08

at the data in more detail, certain aspects merit comment. First, the calculated *d* spacings are all slightly higher than those observed. This reflects the fact that we have assumed maximum lengths for the monomer residues, which will not be the case when there is any nonlinearity, as must occur in an actual chain. Secondly, the calculated peak at $2\theta = 43°$ ($d = 2.12$ Å) is very sharp and invariant. This maximum is the third-order of the HBA length (6.35 Å) and the eighth-order of the TPA–BP dimer length (17.01 Å) and hence is seen for all monomer ratios. This calculated half width is much less than that observed but is increased by consideration of chains with a distribution of monomer axial lengths, as will be discussed below.

When we convert from point to atomic monomers, it can be seen that the meridional peaks are predicted in essentially the same positions. Indeed, the agreement is improved in that we now resolve a peak in the 2.9-Å region. (No such peak is resolved for the point model, although the peak at $d \cong 3.2$ Å is asymmetric, suggesting a weak component at lower *d* spacing.) Visual inspection of the fiber diagrams shows that the intensity agreement is also reasonable, in that the first and second peaks are very weak compared to those at $d \cong 3.2$ and 2.1 Å. Note that in Figure 6, the peak at $d \cong 2.1$ Å has been truncated so that only ~6% of the peak height is shown. Furthermore, the first peak in the calculated data has a much broader profile than the second, as is observed.

The observed and calculated intensities are compared by study of the diffractometer data and the densitometer scans of the film data. Curve c in Figure 7 shows a $\theta/2\theta$ diffractometer scan in the meridional direction for the 50/25/25 composition; the specimen used was the core of the molded plaque. Curve a shows the calculated data for this composition. It can be seen that the relative intensities in the 3-Å region match reasonably well. In the 6-Å region, the first peak is not resolved in the diffractometer scan, and the second peak is clearly more intense than that calculated. From our work on copoly(HBA/TPA/DHN) we know that the intensities in the 6-Å region are very sensitive to the molecular model chosen for the monomers. These intensities are weak because the $F_{AB}(Z)$ terms in eq 8 have minima in this region. Modification of the molecular model, e.g. by tilting the *average* monomers relative to the fiber axis to take account of nonlinearity of the chain, shifts these minima and can increase the intensity of the second peak relative to that of the first. However,

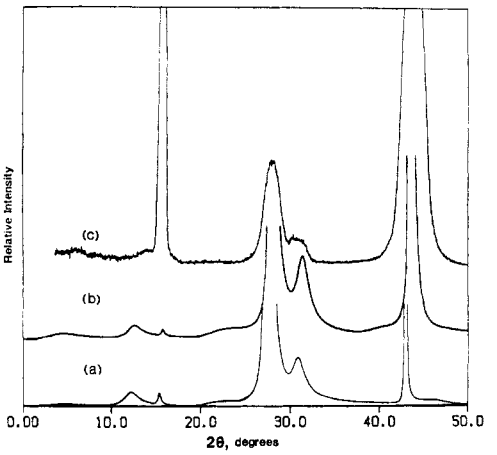

Figure 7. Observed and calculated meridional intensity data for 50/25/25 copoly(HBA/TPA/BP): (a) calculated data for an atomic model with constant residue lengths; (b) calculated data for an atomic model using a distribution of residue lengths shown in Figure 9; (c) observed data from a $\theta/2\theta$ diffractometer scan of a molded plaque along the meridional direction.

we believe that the observed intensity discrepancy is more likely to be due to the development of three-dimensional order. The present one-dimensional calculations assume a nematic structure, whereas the X-ray data indicates that the chains are packed in some type of register, at least in parts of the specimen. Our analyses of the three-dimensional structure in copoly(HBA/HNA) as described elsewhere[11] predict effects comparable to the observed intensification of certain meridional maxima.

The other obvious discrepancy between curves a and c in Figure 7 is in the width of the peak at $d \cong 2.1$ Å. The calculated peak is sharp due to the fact that it is an invariant Bragg peak. The finite half width of 0.006° (2θ) is due to the fact that the ratio of lengths of the HBA residue and the TPA–BP dimer is only approximately (i.e. not exactly) integral (~3:8). The calculated peak has been truncated, and the actual integrated intensity is closer to that observed than it appears at first glance.

In the diffractometer data, some of the width of the 2.1-Å peak is due to instrumental effects. A truer representation of the meridional intensity is obtained by taking densitometer scans of the film data recorded with the specimen tilted for each successive meridional maximum.

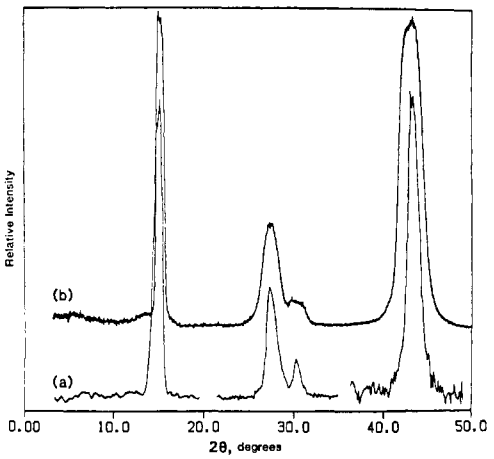

Figure 8. (a) Intensity profiles of meridional maxima at the 6-, 3-, and 2-Å regions for the molded 50/25/25 copoly(HBA/TPA/BP) plaque obtained by densitometer scans of the X-ray film data with the specimen tilted at the approximate Bragg angles. (b) Observed meridional intensity from a $\theta/2\theta$ diffractometer scan of the molded plaque.

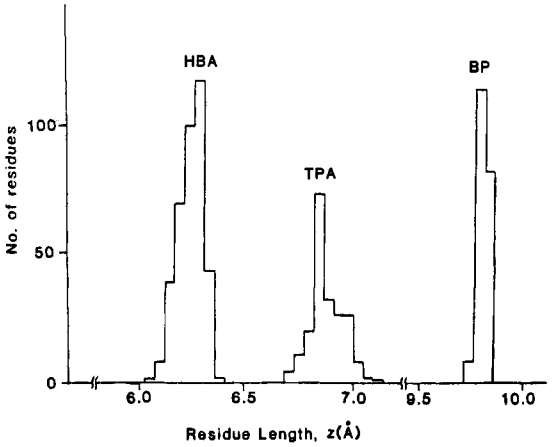

Figure 9. Histograms of axially projected lengths of the comonomers in chains of 50/25/25 copoly(HBA/TPA/BP). This distribution was generated by considering 50 chains of 16 comonomers each.

(Even then, some of the peak width is due to molecular disorientation.) Figure 8, curve a, shows these densitometer scans for the 6-, 3-, and 2-Å regions, taken from film data for the molded plaque interior tilted at the approximate Bragg angle. The three separate scans have been placed on approximately the same scale, based on the exposure time. It can be seen that the 2.1-Å peak is much narrower in the densitometer data. The width at half height is 1.4°, which would yield a crystallite size of 70 Å using the Scherrer equation. As has been discussed previously,[5] the invariant peak can be treated as a Bragg reflection from a limited lattice. The 70-Å "crystallite size" is a measure of the correlation length for the extended chain conformation.

The discrepancy in peak width arises (at least in part) from the fact that the model used for the chain is idealized in a fully extended conformation. Figure 9 shows a histogram of actual residue lengths derived from a survey of 50 chains of 16 monomers for the 50/25/25 copolymer set up using random monomer sequences. Construction of such a series of chains requires assumptions to be made with regard to the conformation: we assumed that the phenyl–ester torsion angles would be ±30° or ±150° (0° and 180° correspond to all planar conformations). The torsion angles were selected at random, but we required that there be approximately equal numbers (±2) of |30°| and |150°| angles. This led to relatively extended conformations, but we also required that all the atoms of an individual chain should lie within a cylinder of diameter 12 Å. This is somewhat arbitrary, but without such a restriction, a random monomer sequence can become appreciably nonlinear after 10 monomers, whereas the results so far indicate that the chain must be almost, if not completely, extended. It seems likely that the forces leading to liquid crystallinity also force the adoption of an extended conformation, just as the converse is true. The distribution of residue lengths in Figure 9 is broadest for TPA and narrowest for BP, with HBA intermediate. This arises largely for the way the monomers are defined, i.e. for ester oxygen to ester oxygen. If the monomers were defined from the center of the C–O(ester) bond, then the distributions for the three residues would be more similar. (This would ultimately lead to generation of the same chain and hence the same intensities.)

When the residue distribution is incorporated into the calculations of $I(Z)$, the results for an atomic model of the 50/25/25 copolymer are shown in Figure 7b. It is immediately apparent that incorporation of the distribution of residue lengths has broadened the peak at 2.1 Å, without having any major effects on the peaks at higher d (lower 2θ). Table I shows the d spacings of the predicted peaks. The changes are minor and in fact are all in the right direction. Previously the calculated d spacings were slightly higher than those observed: use of the length in distribution leads inevitably to shorter average residue lengths, and this results in a shift of all the peaks to slightly higher angles. The agreement now is well within experimental error. Table I also shows the equivalent data for other compositions. These were derived by using the length distributions for the 50/25/25 copolymer, which is not entirely justified but is probably an adequate approximation. It can be seen that the agreement for the d spacings is also improved for each composition.

The use of monomer length distributions has improved our ability to predict the intensity distribution. In particular, the width of the peak at d = 2.1 Å is increased from 0.006° (2θ) for fixed lengths to 0.09°. At the same time, the peak height declines by a factor of 15, such that the integrated peak intensity remains approximately the same. However, it is clear that further refinement of the model is necessary in order to increase the calculated width, which is still an order of magnitude less than the observed value of 1.4°. (Note however, that some of this observed width is due to molecular disorientation, which results in smearing of the layer line streak.) We conclude that the polymer chains are more nonlinear than those considered so far and that the constraints on the torsion angles and overall chain diameter need to be relaxed further, so as to broaden the length distributions for the monomers. This refinement of the model is currently in progress, and we are also modifying the atomic coordinates consistent with nonlinearity of the chain to see if we can improve the match in the 6-Å region. In addition, we are extending our analyses to the three-dimensional structure, where the effects of chain packing are included.

Sensitivity of the X-ray Data to Nonrandomness. It is clear at this point that the nematic random copolymer model gives very good agreement with the observed diffraction data. Such defects as remain are only minor details. No independent information is available on the actual sequence distribution: NMR methods cannot be used due to insolubility of the polymer. Thus it is necessary to address the sensitivity of the data to nonrandomness. This can be done by modifying the monomer

Table II
Effect of Nonrandomness of the Peak Positions of Meridional Maxima for 50/25/25 Copoly(HBA/TPA/BP)

r_H/r_C	d spacings (Å)										
100	17.01	8.51	6.35	5.67	4.25	3.40	3.17	2.84	2.43	2.12	1.89
10	17.02	8.49	6.35	5.68	4.25	3.40	3.18	2.84	2.43	2.12	1.89
5	17.05	8.44	6.38	5.72	4.25	3.38	3.19	2.84	2.43	2.12	1.89
3	17.12	8.32	6.44	5.84	4.24	3.34		2.85	2.43	2.12	1.90
2.0	17.28	8.04	6.66	5.91	4.22	3.31		2.87	2.43	2.12	1.91
1.8	17.86	7.87	6.88	5.91	4.21	3.31		2.89		2.12	
1.6	17.87	7.67		5.92	4.20	3.31		2.90		2.12	
1.4	18.53	7.53		5.93	4.17	3.30		2.93		2.12	
1.2	19.62	7.48		5.93	4.13	3.30		2.94		2.12	
1.0	22.23	7.45		5.93		3.30		2.95		2.12	
obsd											
d		~7.3		5.82		3.20		2.90		2.05	
2θ		(12.1°)		(15.2°)		(27.9°)		(30.8°)		(44.2°)	

sequence statistics, via alteration of the r_{BB} terms in the **M** matrix.

We have considered a simple model in which the B–B, D–D, T–P, and P–T reactions that produce homopoly(HBA), and the alternating copoly(TPA/BP) are more likely than the four cross-reaction B–T, T–D, D–P, and P–B, which are all assumed to have the same probabilities, i.e.

$$r_{BB} = r_{DD}$$

$$r_{TP} = r_{PT}$$

$$r_{BT} = r_{TD} = r_{DP} = r_{PB}$$

These r_{AB} terms are normalized such that $\sum_B r_{AB}p_B = 1$, and the homopolymer terms are related through

$$r_{TP} = \frac{p_T - p_B - r_{BB}p_B^2}{p_T^2}$$

We then define a ratio r_H/r_C as a measure of blockiness, where

$$r_H/r_C = r_{BB}/r_{BT}$$

It is of course debatable whether these probabilities will be equal or whether the first nearest-neighbor probabilities will be independent of the second and third nearest neighbors, but the present model is a good starting point for consideration of the effects of blockiness.

Figure 10 shows plots of $I(Z)$ for the 50/25/25 composition calculated for the random copolymer ($r_H/r_C = 1$) and for nine blocky compositions up to $r_H/r_C = 100$. It can be seen that blocky composition leads to shifts in the peaks that are predicted for the random structure and to the development of new peaks. The peak position for a wider range of r_H/r_C ratios are listed in Table II. When $r_H/r_C = 100$, the structure is extremely blocky, and maxima are predicted at orders of 6.35 and 17.01 Å, which correspond to the repeats for the blocks of poly(HBA) and poly(TPA/BP). Essentially the same peaks are seen at $r_H/r_C = 10$ and 5: the peak widths increase with decreasing r_H/r_C, reflecting the fact that the homopolymer blocks get shorter as cross-reaction becomes more likely. As r_H/r_C is decreased to 3 and 2, the peak positions begin to change, but the calculated data are easily distinguished for those observed. Figure 10 shows equivalent data between $r_H/r_C = 2.0$ and 1.0, where the changes become less obvious. The peaks at 5.92, 3.30 and 2.12 Å remain constant. There is a small shift in the peak at 2.95 Å (to 2.88 Å) and a larger shift in the peak at 7.47 Å (to 8.00 Å). These data were obtained by using constant residue lengths, but the same sort of effects would be expected if we incorporated the length distribution function.

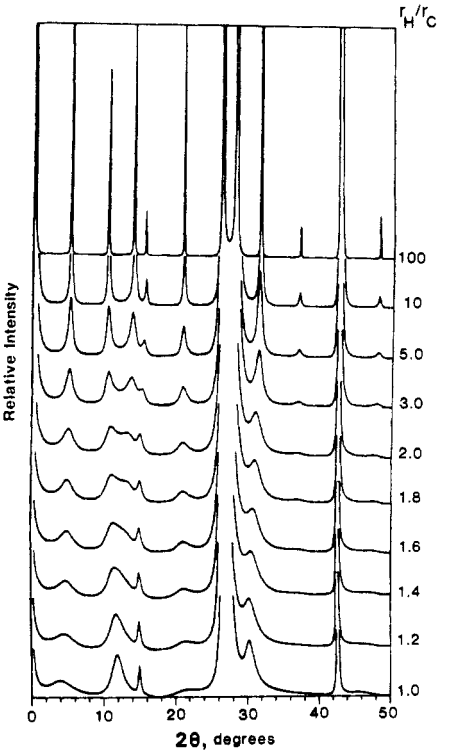

Figure 10. Calculated meridional intensities of an atomic model of 50/25/25 copoly(HBA/TPA/BP) chain at different degrees of blockiness defined by the ratio r_H/r_C. The random copolymer corresponds to $r_H/r_C = 1$.

Thus we predict a shift of 0.5 Å for the first peak for the 50/25/25 copolymer as blockiness is increased from random to $r_H/r_C = 2.0$. Unfortunately this peak is weak and diffuse and difficult to measure to an accuracy better than ±0.2 Å using the film data. Hence we can rule out nonrandomness for $r_H/r_C \geq 1.6$, based on the peak positions. In comparison, the first peak for copoly(HBA/HNA) is predicted to shift by 0.7 Å over the same range and is sharper and more intense, and we can rule out $r_H/r_C \geq 1.4$. However, for the present polymer we predict a peak at 4.17 Å for $r_H/r_C = 1.4$ which is not detected in the observed data, and hence we can extend the limits to the latter figure. Note that, at $r_H/r_C = 1.4$, there is still significant nonrandomness: for example, the possibility of $(HBA)_4$ units is 1.59 times greater than in the random copolymer. Nevertheless, the proportion of homopolymer blocks is still very low, and the high crystallinity observed cannot be due to just these sequences; rather it must involve crystallization of random sequences.

Hence we are able to use X-ray methods to rule out blocky structures, at least within the limits defined above,

with $r_H/r_C \geq 1.4$. This is a significant observation, since we are currently unable to investigate sequence distribution by NMR methods. The conclusion that the polymer is at least close to having a completely random structure is interesting in view of the fact that the monomers probably have different reactivities and that TPA is insoluble in the initial synthesis mixture. It seems likely that transesterification will randomize the copolymer at a relatively early stage of the synthesis, perhaps after the formation of oligomers.

Acknowledgment. This research was supported by NSF Grant No. DMR84-17525 and by Dartco Manufacturing Inc. We are indebted to Dr. N. D. Field and his colleagues at Dartco, Augusta, GA, for synthesizing and processing the specimens of the copolymer in the form of as-spun and annealed fibers and also molded plaques.

Registry No. (HBA)(TPA)(BP) (copolymer), 31072-56-7.

References and Notes

(1) Wood, A. S. *Mod. Plast.* **1985**, April, 78.
(2) "Plastiscope", *Mod. Plast.* **1984**, Dec, 14.
(3) Gutierrez, G. A.; Chivers, R. A.; Blackwell, J.; Stamatoff, J. B.; Yoon, H. *Polymer* **1983**, *24*, 937.
(4) Blackwell, J.; Biswas, A. *Macromolecules* **1985**, *18*, 2126.
(5) Blackwell, J.; Biswas, A. *Macromol. Chem.—Macromol. Symp.* **1986**, *2*, 21.
(6) Blackwell, J.; Cageao, R. A.; Biswas, A. *Macromolecules*, in press.
(7) Mitchel, G. R.; Windle, A. H. *Colloid Polym. Sci.* **1985**, *263*, 230.
(8) Blackwell, J.; Gutierrez, G. A.; Chivers, R. A.; Ruland, W. *J. Polym. Sci., Polym. Phys. Ed.* **1984**, *22* 1343.
(9) Bonart, R. C.; Blackwell, J.; Biswas, A. *Makromol. Chem., Rapid Commun.* **1985**, *6*, 353.
(10) Field, N. D. *Polym. Process. Soc.* **1986**, Montreal, April.
(11) Biswas, A.; Blackwell, J., manuscript in preparation.

Side-Chain Effects on Ultraviolet Absorption of Organopolysilane Radical Anions

Hiroshi Ban* and Ken Sukegawa

NTT Electrical Communications Laboratories, Tokai Ibaraki 319-11, Japan

Seiichi Tagawa

Research Center for Nuclear Science and Technology, University of Tokyo, Tokai Ibaraki 319-11, Japan. *Received June 2, 1987*

ABSTRACT: Eight kinds of organopolysilane radical anions in tetrahydrofuran solution were investigated utilizing the pulse radiolysis technique. UV absorption maxima of poly(alkylsilane) radical anions are observed at 355–363 nm. Introducing a methylphenylsilylene unit or diphenylsilylene unit into the polymer chains causes a slight red shift in the UV absorption of their radical anions. This can be understood on the basis of an electronic interaction between the silicon main chain and pendant phenyl groups. Extinction coefficients of these radical anions were determined to be 1.4–2.1 × 10^5 per mol of added electron.

Introduction

In our previous report, high molecular weight organopolysilane radical anions were first observed by utilizing the pulse radiolysis technique with 2-ns time resolution.[1] Poly(methylpropylsilane) (PMPrS) and poly(methylphenylsilane) (PMPS) radical anions in tetrahydrofuran (THF) solutions were investigated, and their optical properties and kinetics were discussed. On the other hand, cyclic organopolysilane radical anions such as $(Si(CH_3)_2)_n$ (n = 4–6) and $(Si(C_6H_5)_2)_m$ (m = 4, 5) have been already observed by reduction with alkali metal.[2-5] ESR studies have shown that unpaired electrons of these cyclic radical anions are delocalized over the ring skeleton.[3,5] Added electrons of PMPrS and PMPS radical anions are also considered to delocalize along the catenating silicon chain.

Organopolysilane solid films reveal high electric resistance but become p-type semiconductors in the presence of strong electron acceptors such as AsF_5 or SbF_5.[6] This may suggest that catenating silicon atoms of organopolysilane molecules can be essentially a semiconducting path. Ionic or charge-transfer states are often related to electric properties. Study of polysilane radical anions is of interest from the viewpoint of the potential semiconductivity of the silicon chain. The pulse radiolysis technique is very useful in that the dynamic behavior of polysilane radical anions can be observed.

Organopolysilanes have strong absorption bands in the 300–360-nm region. Absorption peaks (λ_{max}) of poly(alkylsilanes) are usually found at 300–320 nm, which have been attributed to a transition from the highest occupied silicon σ orbital to the σ^* orbital.[7] However, λ_{max}'s of poly(arylsilanes) such as PMPS or diphenylsilane copolymers occur at 340–360 nm.[8] This red shift indicates the contribution of π–σ^* character for the transition according to the aryl substituents.[7,9,10] Similar electronic interaction between the silicon main chain and aryl substituents can be anticipated for polysilane radical anions. In this report, eight other kinds of polysilane radical anion in THF solutions are investigated by pulse radiolysis, and side-chain effects on their optical properties are discussed.

Experimental Section

The following polymers were synthesized according to the conventional method:[11-13] poly(β-phenethylmethylsilane) (PPnMS); poly[(dimethylsilane)-*co*-(methylcyclohexylsilane)] (DMS–MHxS); poly[(dimethylsilane)-*co*-(methylpropylsilane)] (DMS–MPrS); poly[(dimethylsilane)-*co*-(β-phenethylmethylsilane)] (DMS–PnMS); poly[(dimethylsilane)-*co*-(methylphenylsilane)] (DMS–MPS); poly[(diphenylsilane)-*co*-(dimethylsilane)] (DPS–DMS); poly[(diphenylsilane)-*co*-(methylpropylsilane)] (DPS–MPrS); poly[(diphenylsilane)-*co*-(β-phenethylmethylsilane)] (DPS-PnMS). Molar monomer feed ratios of these copolymers were fixed to 1:1. Molecular weights were determined by gel permeation chromatography (GPC). Compositions of these copolymers were determined by ^1H NMR signal intensities, except DMS–MHxS and DMS–MPrS, whose compositions were determined by ^{13}C NMR. Their compositions and molecular weights are listed in Table I.

0024-9297/88/2221-0045$01.50/0